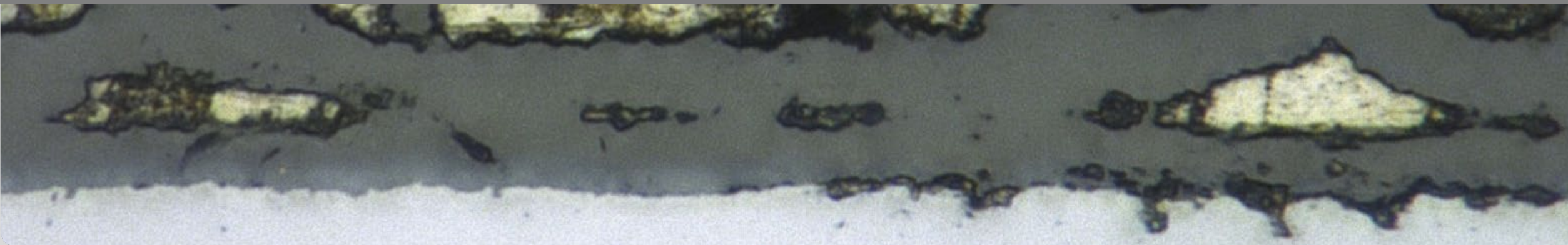


Oxidation kinetics at 450–550 °C for Steel T91 in flowing lead–bismuth eutectic (2 m/s, 10⁻⁶ % oxygen)

Carsten Schroer, Aleksandr Skrypnik, Olaf Wedemeyer, Valentyn Tsisar*

Institute of Applied Materials – Applied Materials Physics (IAM-AWP)

*SCK•CEN, Mol, Belgium



WHY LEAD–BISMUTH EUTECTIC?

Renewed interest in liquid lead/lead alloys as a coolant for nuclear applications

Lead-cooled fast reactor (Gen VI).

Accelerator driven system.

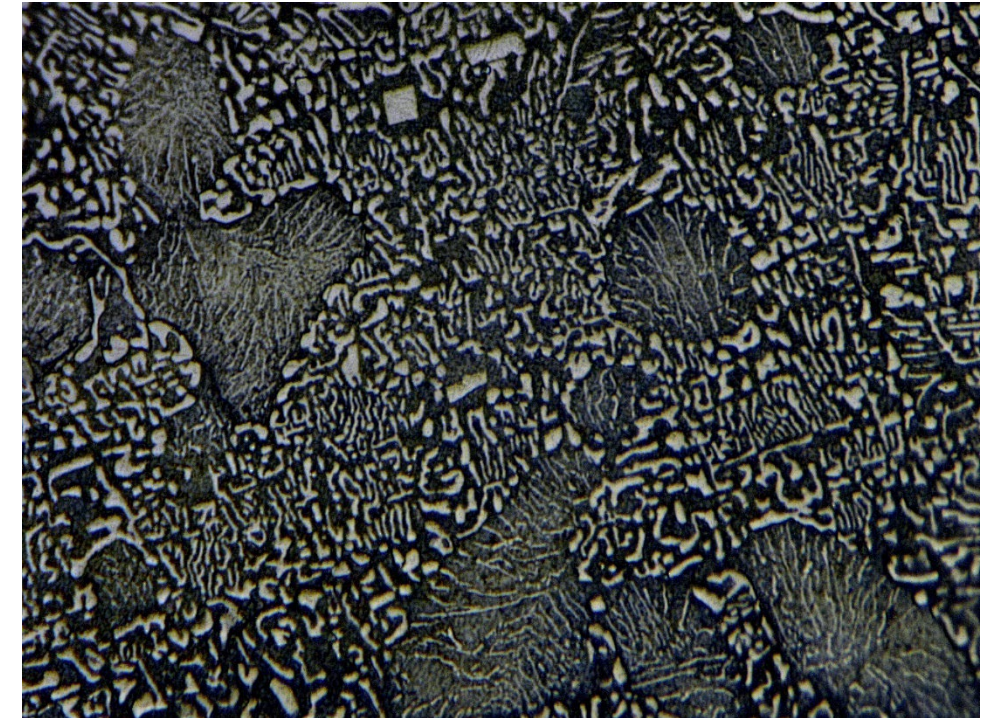
Low melting point of lead–bismuth eutectic (LBE) attractive for first-of-their-kind installations

127.5 vs. 327.5 °C for pure lead (Pb).

However, specific disadvantages to application on industrial scale

Polonium production.

High price of bismuth (Bi).



100 μm

OXIDATION IN LIQUID METALS

Natural corrosion mode of metallic materials in contact with liquid metals is dissolution

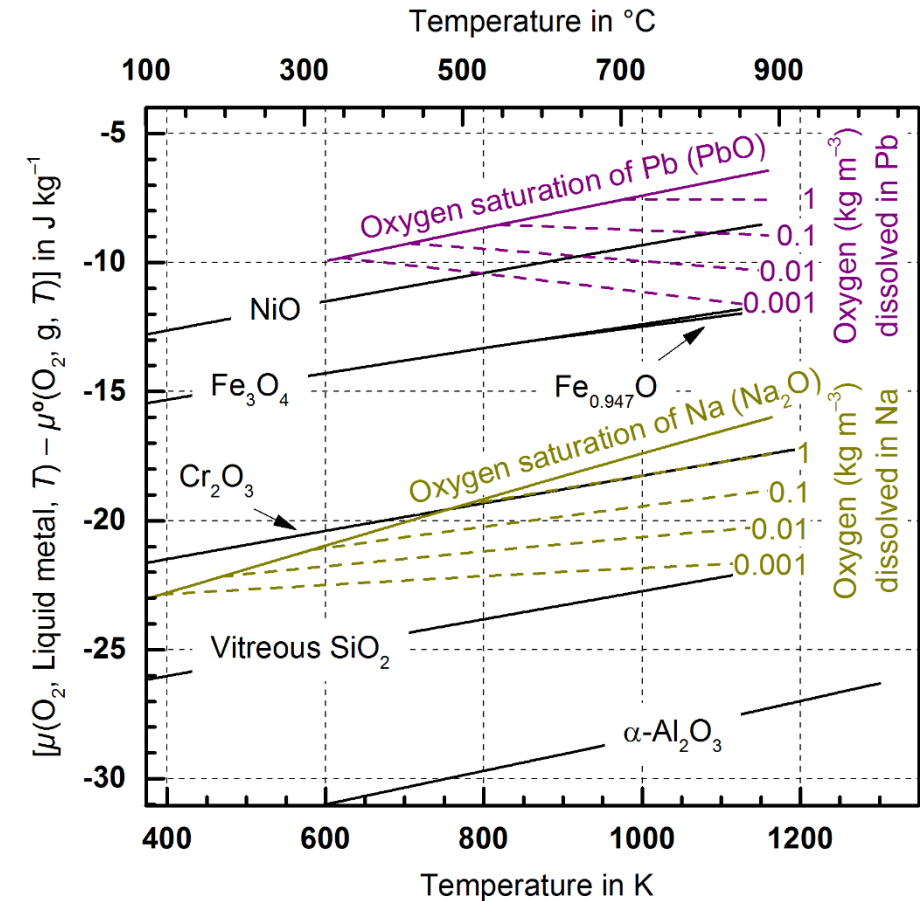
Occasionally small, but generally non-zero solubility of the constituent elements of solid metals and alloys.

However, the liquid metal may act chemically more noble than major elements of the solid

E.g. for Pb (or LBE) in comparison with steel, to much lower degree in the case of sodium (Na).

Persistent oxide scale typically requires continuous oxygen addition

Reduced element dissolution through separation from the liquid, but possibly at the cost of material functionality.



Sources of thermochemical data: Pankratz, *Thermodynamic properties of elements and oxides*, 1982; Noden, *J. Brit. Nucl. Ener. Soc.*, 1973 (oxygen solubility in Na); Ganesan et al., *J. Nucl. Mater.*, 2006 (oxygen solubility in Pb).

FERRITIC/MARTENSITIC STEEL T91

One of the early candidate materials for nuclear application of liquid Pb/LBE

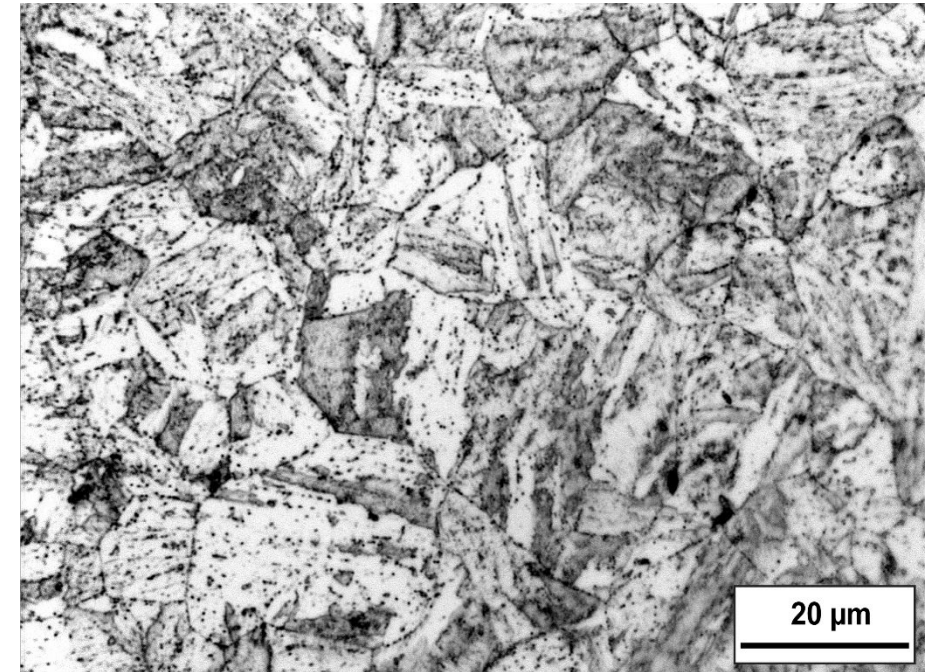
Interest for currently planned pilot plants has cooled down, but T91 still being used as a reference for material studies.

Respectively high availability of data for interaction with Pb/LBE at various conditions

Temperature, flowing/static liquid metal, dissolved oxygen concentration, exposure time, without/with mechanical load.

Exploitable for fundamental understanding of steel performance in oxygen-containing liquid

E.g. Simultaneous oxidation and dissolution at low oxygen activity.



Microstructure of 9Cr-1Mo ferritic/martensitic steel T91.

FOCUS OF THE TALK

Source of oxidation data for T91

Qualitative and quantitative results from exposure tests in the CORRIDA loop identified as representing oxidation.

Nominal conditions of 450–550 °C, 2 m/s flowing LBE, 10^{-6} % dissolved oxygen

Aspects of oxidation mechanisms

Elementary subprocesses and their sequence.

Kinetics of material degradation

Rate laws reflecting the observed progress of material consumption.

Estimate of activation energy

As resulting from Arrhenius plot.



LBE-loop CORRIDA operated at KIT.



Ø8×35 mm samples for exposure to flowing LBE.

EXPERIMENTAL BASIS OF THE PRESENTED WORK

550 °C, 2 m/s LBE, 10⁻⁶ % oxygen
+5 °C and ±0.2 m/s temperature and flow
variation, respectively.

1.4/1.6×10⁻⁶ % average oxygen concentration.

~385 °C cold-leg temperature of the LBE loop.

T91-A: ~5000–20,000 h.

T91-B: ~500–15,000 h.

450 °C, 2 m/s LBE, 10⁻⁶ % oxygen

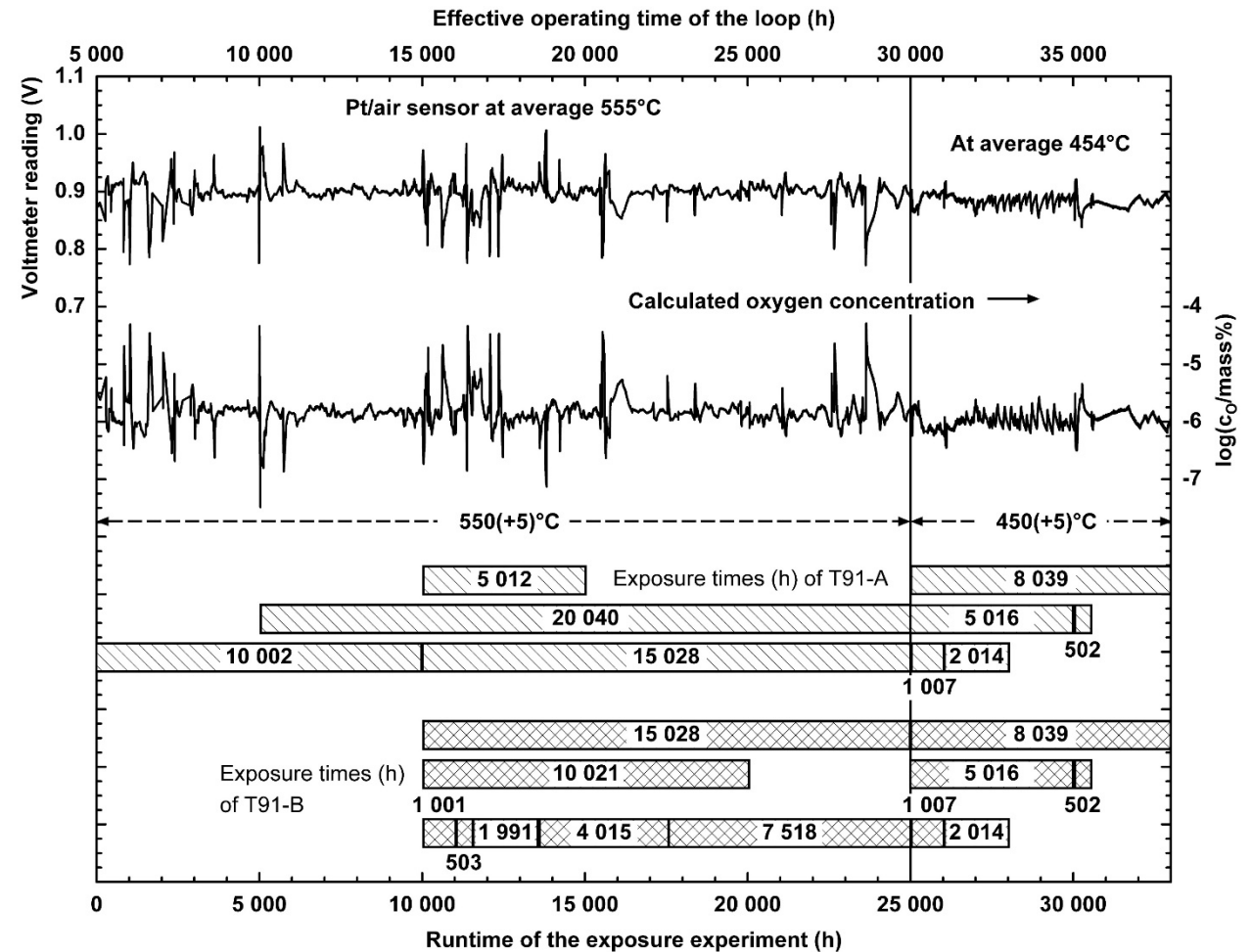
+5 °C and ±0.2 m/s temperature and flow

variation, respectively.

1.1×10⁻⁶ % average oxygen concentration.

~300 °C cold-leg temperature.

T91-A, T91-B: ~500–8000 h.



Exposure chart for tests at 550 and 450 °C including representative oxygen sensor reading and calculated concentration of oxygen dissolved in the flowing LBE.

Schroer et al., Nucl. Eng. Des., 2014.

EXPERIMENTAL BASIS OF THE PRESENTED WORK

500 °C, 2 m/s LBE, 10^{-6} % oxygen

+7 °C temperature variation.

Flow velocity gradually decreasing from 2 to 1.6 m/s.

1.2×10^{-6} % average oxygen.

~325 °C cold leg temperature.

T91-B, T91-C: 504, 1007, 2016 h.

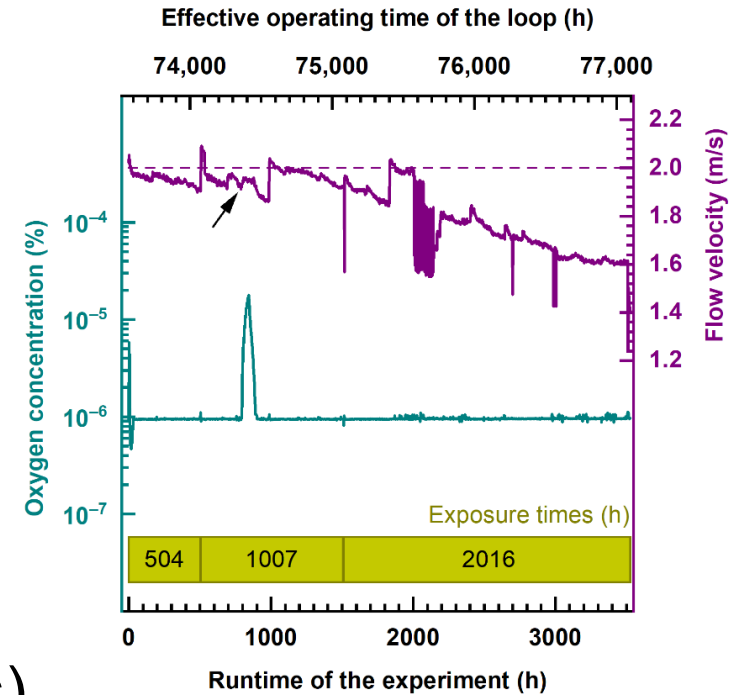
2.0 ± 0.2 1.8 ± 0.2 m/s

Post-test examinations (all temperatures)

Cross section analysis in the light-optical (LOM) and scanning-electron microscope (SEM).

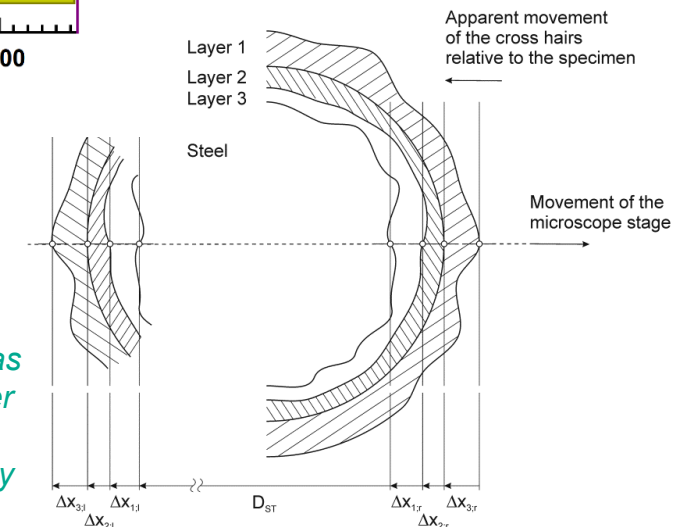
Energy dispersive X-ray spectrometry (EDS).

Assessment in the LOM of corrosion scale thickness and consumption of the material.

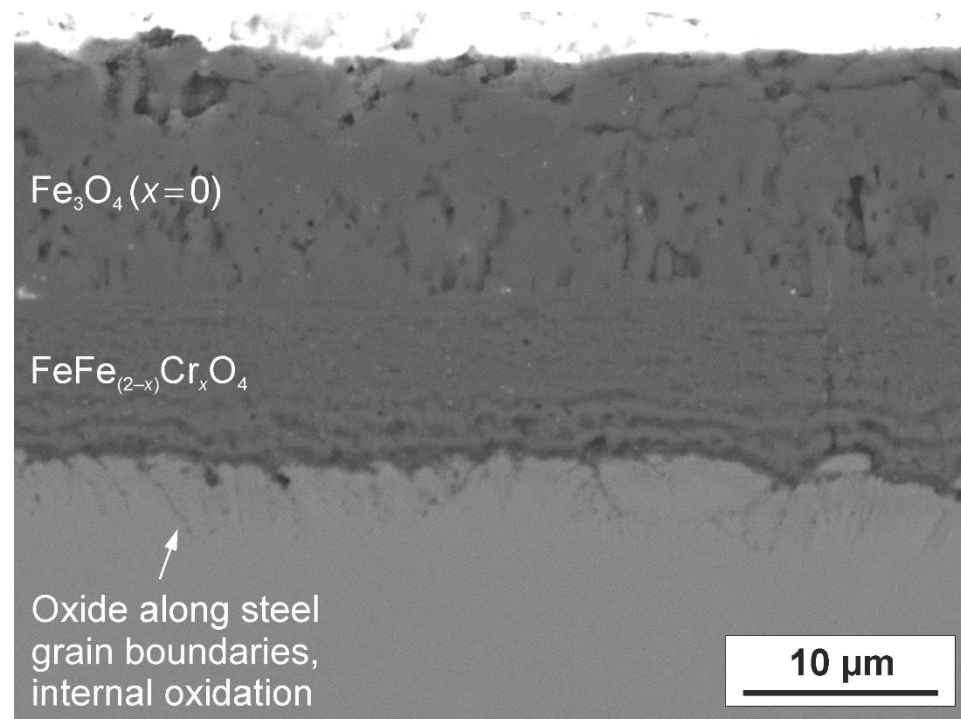


Oxygen concentration and flow velocity along the cylindrical samples during the exposure test at 500 °C.

Measurement of the thickness of distinguishable corrosion layers as well as the material diameter after the test (for comparison with the diameter before the test), typically 24 and 12 times, respectively.



GENERAL STRUCTURE OF THE OXIDE SCALE



T91-B after exposure for 8039 h at 450 °C.

Magnetite (Fe_3O_4) at the interface with LBE
May be missing under conditions promoting solution of iron (Fe).

Spinel ($\text{FeFe}_{(2-x)}\text{Cr}_x\text{O}_4$)
Typically heterogenous layer indicating variable x .
Average $x \approx 0.6$ expected in view of steel composition.

Internal oxidation zone (IOZ)
 x in spinel approaching 2 (chromite, FeCr_2O_4) or chromia (Cr_2O_3)?
Generally less pronounced at low temperature.

ORIGIN OF THE TYPICAL OXIDE SCALE

Natural/initially formed oxide, protective to some degree

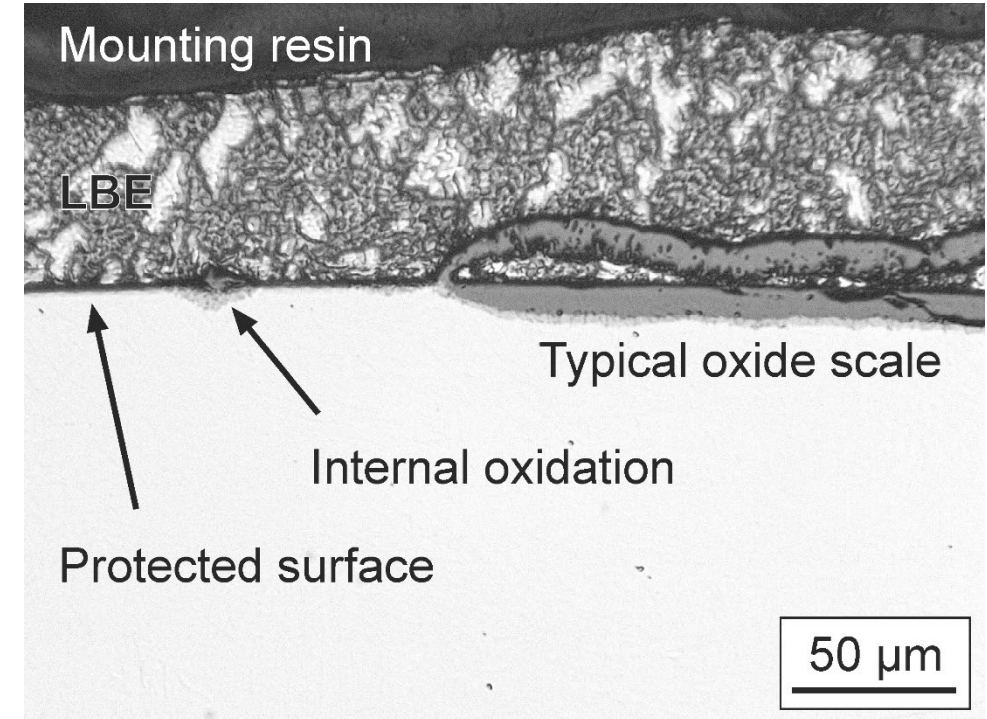
Likely to be chromium- (Cr) rather than Fe-rich.
 Prone to failure because of small but non-zero solubility in LBE (solubility product of metal component and oxygen).
 Either solution of the steel or accelerated oxidation subsequent to failure of the protective scale failure.

Internal oxidation may dominate the early stage of accelerated oxidation

Especially at 500 and 550 °C.
 Steel likely to be depleted in Cr at this stage.

Development of scale through lateral growth

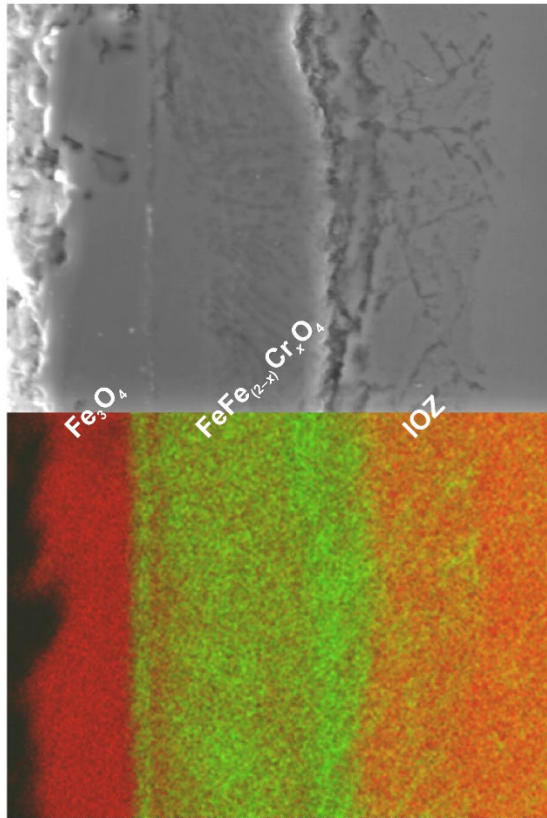
The more so the fewer the sites of failure of the once protective scale.



T91-C after exposure for 2016 h at 500 °C.

Incubation time of the scale likely to be noticeable in oxidation kinetics

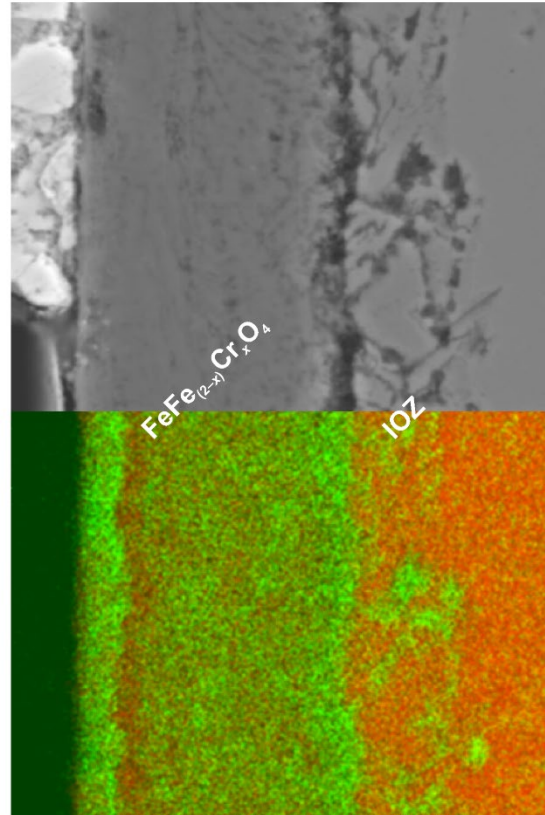
DETAILS OF SCALES FORMED AT 550 °C



Red: Iron
Green: Chromium

10 µm

T91-A after 1200 h at 550 °C with $>10^{-6}$ % oxygen in flowing LBE during the first half of the exposure.



Red: Iron
Green: Chromium

10 µm

T91-B after exposure to flowing LBE for 1001 h at 550 °C and 10^{-6} % oxygen.

Cr- and Fe-rich sublayers at magnetite/spinel interface or spinel surface

Seem to corroborate origination from Cr-rich initial scale with Cr-depleted steel underneath.

Plain re-ordering of Fe and Cr in non-equilibrium spinel would result in reverse order of Cr- and Fe-rich sublayers (*Whittle and Wood, J. Electrochem. Soc. 114, 1967*).

Substructure in the spinel volume reminiscent of IOZ

Cr-depleted steel matrix of the IOZ consumed by formation of spinel that encloses the Cr-rich internal oxide.

Dynamic rather than steady-state substructure of the spinel layer

DETAILS OF SCALES AT 450 AND 500 °C

Stratified inner part of the spinel

Rather than reminiscence of IOZ.

Relative fine substructure as a result of lower temperature.

No Cr-depleted sublayer underneath Cr-rich spinel at spinel surface

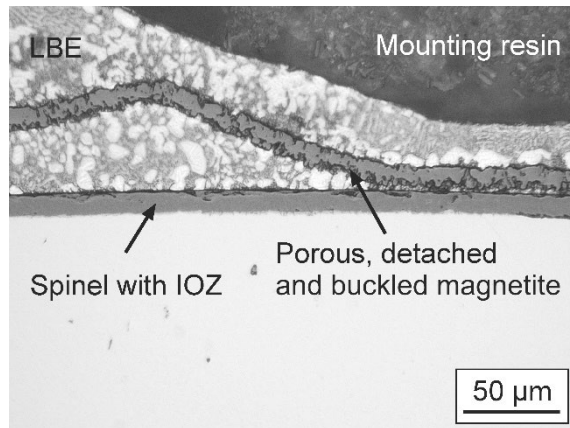
Especially clear for 450 °C at which initial steel depletion is likely to be the least pronounced.

Apparent enrichment of Fe in spinel at the magnetite/spinel interface at 450 °C

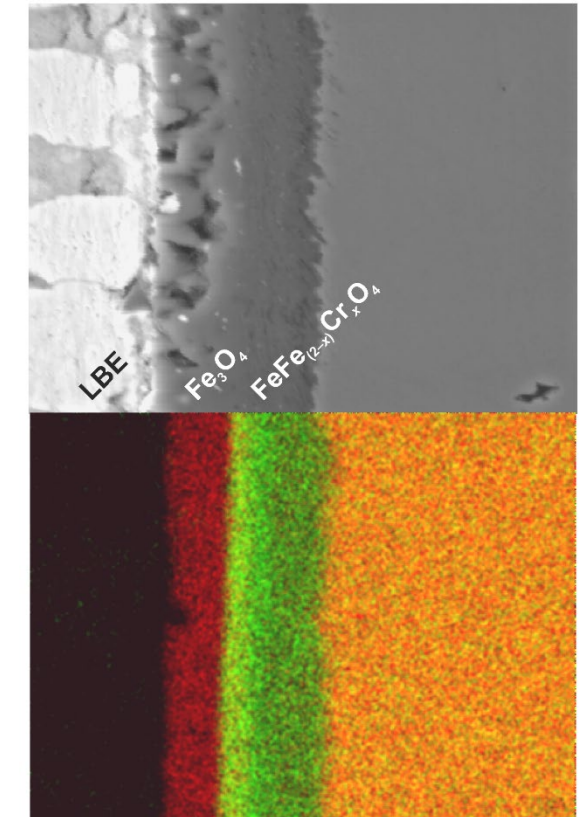
Detachment and buckling of magnetite

More frequent in occurrence at 500 °C.

Continuous Fe diffusion through the magnetite, towards the LBE where Fe activity is lowest; weakening of the magnetite/spinel interface at reduced Fe supply across the spinel.



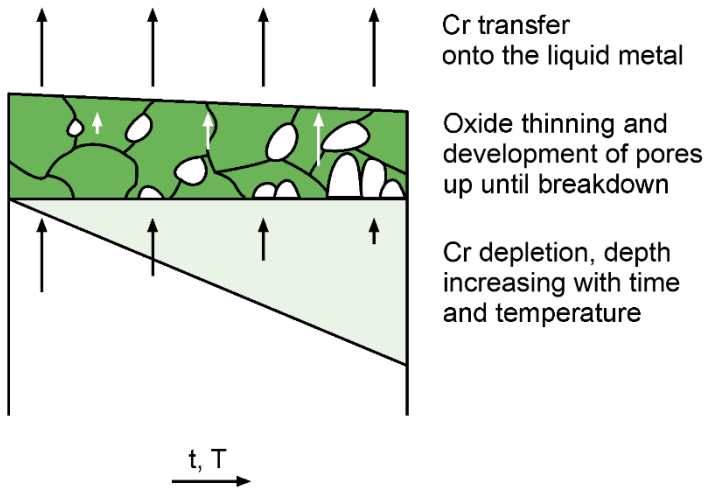
T91-C after 2016 h at 500 °C.



Red: Iron
Green: Chromium

T91-B after exposure to flowing LBE for 1007 h at 450 °C and 10⁻⁶ % oxygen.

ASPECTS OF OXIDATION MECHANISMS



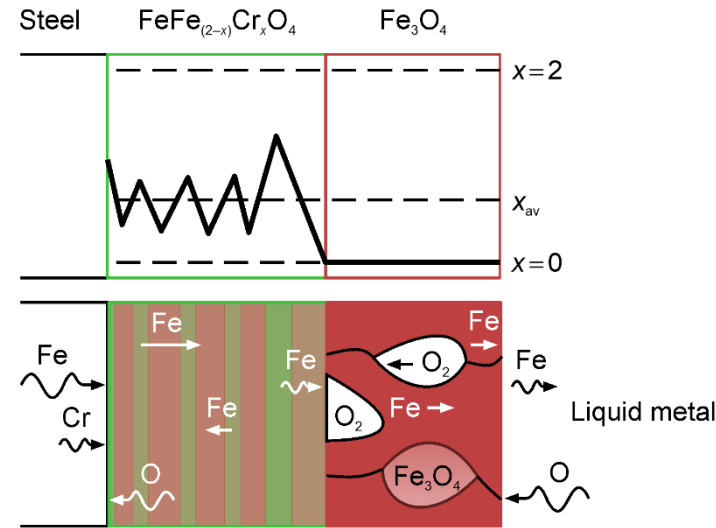
Failure of Cr-rich oxide resulting from small but non-zero solubility

Cr depletion of the steel.

Mass transfer onto the liquid metal satisfied by oxide thinning or from within the oxide.

[1] Whittle and Wood, *J. Electrochem. Soc.* 114, 1967.

[2] Birks, Meier and Petit, *Introduction to the High Temperature Oxidation of metals*, 2006.

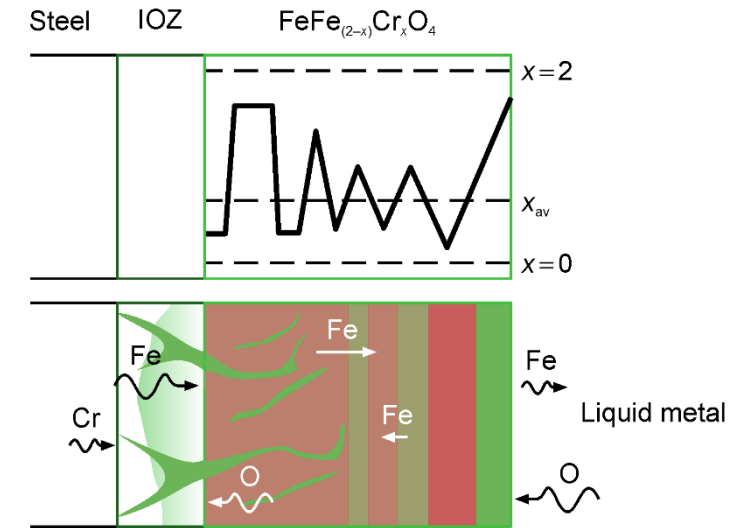


Stratified spinel, magnetite (450 °C)

Variable diffusion coefficients and concentration gradients in the spinel.^[1]

Net transfer of Fe across the spinel.

Detachment and buckling of magnetite through development of porosity and oxide formation on grain boundaries.^[2]



Internal oxidation, no magnetite (550 °C)

Three-dimensional patterning of the spinel.

Spinel especially Cr-rich at the surface with Cr-poor sublayer underneath possibly artefact from once protective oxide.

Fe dissolution alternatively to magnetite formation.

OXIDATION KINETICS

Paralinear rate law

Parabolic oxide growth superimposed by linear recession of oxide or

$$\frac{d\xi}{dt} = \frac{k_p}{2\xi} + k_l$$

with parabolic rate constant k_p , linear rate constant k_l . ξ : scale thickness or recession of unaffected material.

$k_l < 0$ for scale thickness, $k_l > 0$ for associated material consumption.

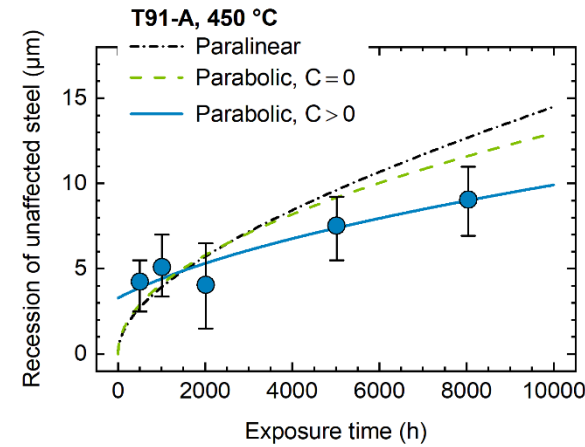
Overestimates the recession of unaffected steel observed for oxidation of T91 in LBE.

Parabolic rate law

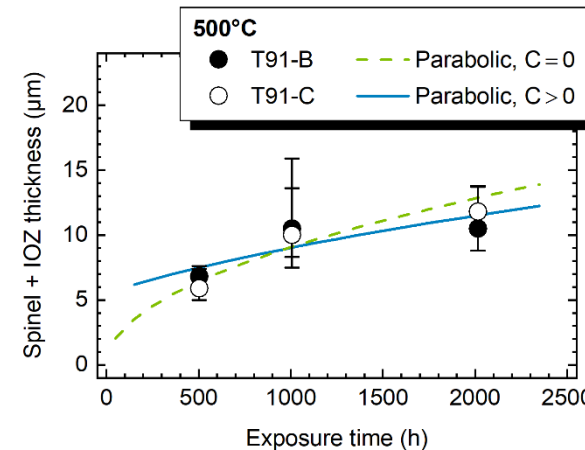
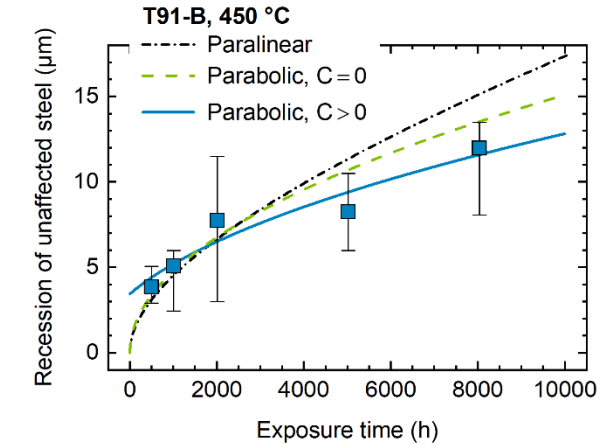
Integration gives

$$\xi^2 = k_p t + C$$

Integration constant $C > 0$ suggests that the progress becomes parabolic at $t > 0$ and $\xi > 0$. With $C > 0$, best fit to steel recession observed at 10^{-6} % oxygen (*Schroer et al., J. Nucl. Mater. 431, 2012; Nucl. Eng. Des. 280, 2014*).



Average loss of T91 on oxidation in flowing (2 m/s) LBE at 450 °C and 10^{-6} % oxygen.



Sum of spinel and IOZ thicknesses used as a substitute for the recession of unaffected steel at 500 °C.

ACTIVATION ENERGY AT 2 m/s AND 10^{-6} % OXYGEN

T (°C)	k_p ($\mu\text{m}^2/\text{h}$)	C (μm^2)	k_p^* ($\mu\text{m}^2/\text{h}$)
450	0,0153	11,8	0,0228
500	0,0505	30,7	0,0821
550	0,0808	536	0,231
k_0 ($\mu\text{m}^2/\text{h}$)	1.67×10^4		4.47×10^6
E_A (kJ/mol/K)	83.0		115

Parameters of parabolic rate laws obtained for T91-B and results of Arrhenius analysis.

Identification of the role of oxygen in oxidation mechanisms possible with this data?

Arrhenius approach to activation energy

$$k_p(T) = k_0 \exp\left(\frac{-E_A}{RT}\right)$$

with pre-exponential factor k_0 and activation energy E_A .

Activation energy 83.0 (115) kJ/(mol K) for T91-B as compared to 97.5 (122) kJ/(mol K) in the case of T91-A (no data at 500 °C for the latter material).

2 m/s and $\sim 2 \times 10^{-7}$ % oxygen

(Tsisar et al., Corros. Sci. 174, 2020)

According to recession of sound steel in T91-B at 400, 450 and 550 °C. Parabolic laws with $C=0$ (k_p^*) generally better fit than $C > 0$, implying that slow-growing initial oxide fails relatively early.

$$k_0^* = 28.8 \times 10^6 \mu\text{m}^2/\text{h}, E_A^* = \underline{133 \text{ kJ}/(\text{mol K})}.$$

Especially the pre-exponential factor, but also activation energy of oxidation seems to increase with decreasing oxygen content of LBE.

APPROACH TO PREDICTING OXIDATION OF T91

Parabolic law for recession of sound steel

$$\xi^2 = k_0(w_O) \exp\left[\frac{-E_A(w_O)}{RT}\right] + C(T, w_O)$$

with mass concentration w_O of oxygen dissolved in LBE.
 C , representing incubation and the development of the typical scale, is a function of temperature and oxygen concentration.

Data for $w_O = 10^{-6}$ % suggests exponential temperature dependence of C .

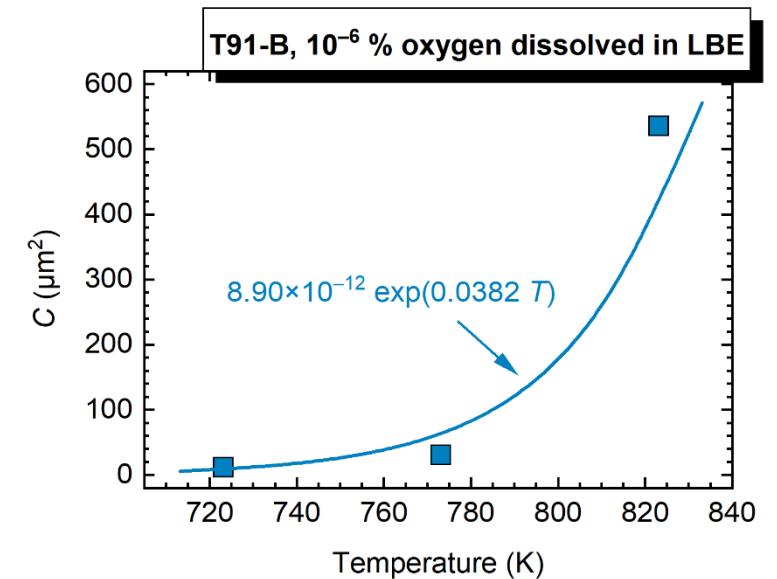
$C = 0$ at $w_O \leq 2 \times 10^{-7}$ % (?).

Dependence of k_0 , E_A and C on w_O ?

Also needed for full description

Associated thickness of oxide layers.

Simultaneous solution of steel elements.



Exponential function fitted to temperature dependence of C at 10⁻⁶ % dissolved oxygen.

Empirical modelling requires at least one additional data set at another oxygen concentration

CONCLUSIONS

Oxidation process relevant to T91 in LBE needs incubation

Incubation time depends on oxygen concentration and temperature.

Complex, temperature-dependent morphology of oxide scale

Especially of the $\text{FeFe}_{(2-x)}\text{Cr}_x\text{O}_4$ layer, suggesting time dependent apparent diffusivity iron and chromium (or oxygen).

Long-term data required for identification of rate laws

> (>>) 2000 h for oxidation of T91 in LBE, two data points at least (?).

Arrhenius analysis of parabolic rate laws for steel recession gives indications as to the influence of temperature and oxygen concentration in LBE

Predictive equation needs additional experiments at another oxygen concentration.

So far evaluated data should suffice corroboration of proposed oxidation mechanisms, especially as concerning the role of oxygen dissolved in LBE.

ACKNOWLEDGEMENTS

Financial support by the Nuclear Waste Management, Safety and Radiation Research Program (NUSAFE) of KIT is gratefully acknowledged.

The experiments performed in the CORRIDA loop received funding from the EURATOM 6th and 7th Framework Program as well as HORIZON 2020.

The authors would like to thank their colleagues of the Institute for Thermal Energy Technology and Safety (ITES) for valuable advice and hands-on support during operation of CORRIDA.

Likewise, the contributions by former staff of KIT is acknowledged.

Oxidation kinetics at 450–550 °C for Steel T91 in flowing lead–bismuth eutectic (2 m/s, 10⁻⁶ % oxygen)

Carsten Schroer, Aleksandr Skrypnik, Olaf Wedemeyer, Valentyn Tsisar*

Institute of Applied Materials – Applied Materials Physics (IAM-AWP)

*SCK•CEN, Mol, Belgium

